Tampere University

Elias Kokko

DEVELOPMENT OF FLUORESCENCE MEASUREMENT SYSTEM FOR AN AUTOMATED MULTI-WELL PLATE ILLUMINATION DEVICE

Faculty of Medicine and Health Technology
Bachelor's Thesis
May 2019

ABSTRACT

Elias Kokko: Development of fluorescence measurement system for an automated multi-well plate illumination device
Bachelor's Thesis, 30 pages
Tampere University
Engineering and Natural Sciences, BSc, Bioengineering
May 2019

During fluorescence, a substance emits light after it has absorbed photons from an excitation light source. The emitted fluorescent light has a longer wavelength than the absorbed light. This phenomenon is utilized extensively in a variety of applications, such as in fluorescence labelling in in-vitro studies and as a diagnostic tool in ophthalmology, due to being a non-destructive and a highly sensitive approach.

The aim of this thesis is to propose a design for a fluorescence measurement system for an automated multi-well plate illumination device, manufactured by Modulight Inc. A measurement setup, which was constructed inside the device, was used to perform fluorescence measurements, the outcome of which determined whether the measurement system design was successful or needed further development. These measurements were carried out using the built setup to excite samples of protoporphyrin IX, a fluorescent compound, and measure its emission spectrum at different concentrations excited with different intensities.

The results of the experimental part of this thesis showed that with the constructed measurement system, it was possible to measure fluorescence emission from the prepared samples. In the light of this, the targets set to this bachelor's thesis were accomplished and the product development of the fluorescence measurement system has proceeded from a design phase to an early prototype phase. In future development, the system can be further improved by reducing the amount of excitation light detected, and by enhancing the collection of fluorescence.

Keywords: fluorescence, fluorescence spectroscopy, illumination device, spectrum

TIIVISTELMÄ

Elias Kokko: Fluoresenssimittausjärjestelmän kehittäminen kuoppalevyjä valottavalle laitteelle
Kandidaatintyö, 30 sivua
Tampereen yliopisto
Tekniikka ja luonnontieteet, TkK biotekniikka
Toukokuu 2019

Fluoresenssin aikana aine absorboi valoa ja emittoi sitä aallonpituuksilla, jotka ovat pidempiä kuin eksitointiin käytetyt aallonpituudet. Tätä ilmiötä hyödynnetään laajalti eri sovelluksissa, kuten in vitro -kokeissa, joissa sitä käytetään esimerkiksi proteiinien fluoresenssimerkkauksessa. Eräs toinen sovelluskohde fluoresenssille on oftalmologia eli silmätautioppi, jossa fluoresenssia käytetään diagnostisena työkaluna. Fluoresenssin etuja muihin menetelmiin verrattuna ovat sen herkkyys ja ei-destruktiivisuus.

Tämän työn tarkoitus on kehittää fluoresenssimittausjärjestelmä Modulight Oy:n valmistamalle kuoppalevynvalotuslaitteelle. Työssä laitteen sisälle rakennettiin mittausjärjestelmä, jolla voitiin mitata näytteistä fluoresenssia. Mittauksista saatujen tulosten perusteella voitiin arvioida, oliko rakennettu järjestelmä käyttökelpoinen. Fluoresenssimittaukset suoritettiin valottamalla eri konsentraatioissa olevaa protoporfyriini IX -yhdistettä eri eksitaatiovalon intensiteeteillä, jolloin yhdisteen emittoimasta fluoresenssista voitiin mitata emissiospektri.

Tulosten perusteella järjestelmän voitiin todeta olevan toimiva, eli sillä pystyttiin havaitsemaan ja mittaamaan näytteen lähettämää fluoresenssia. Näin ollen työ saavutti sille asetetut tavoitteet, ja järjestelmän suunnitteluvaiheesta edettiin prototyyppivaiheeseen. Järjestelmän tuotekehitystä voidaan nyt jatkaa eteenpäin, esimerkiksi vähentämällä eksitaatiovalon havaitsemista ja tehostamalla emittoidun fluoresenssin havaitsemista.

Avainsanat: fluoresenssi, fluoresenssispektroskopia, valotuslaite, spektri

PREFACE

I would like to express my gratitude to Modulight Inc. for giving me the opportunity to carry out my bachelor's thesis. I would like to thank my supervisor Dr. Lasse Orsila, who provided valuable feedback and support during this thesis work. Finally, I would like to thank Dr. Juha Nousiainen for his contribution, providing me with valuable inputs.

Tampere, 13.5.2019

Elias Kokko

CONTENTS

LIST OF FIGURES

LIST OF SYMBOLS AND ABBREVIATIONS

ADC	Analog to Digital Converter
CCD	Charge-Coupled Device
DMSO	Dimethyl Sulfoxide
FC	Ferrule Connector
GFP	Green Fluorescent Protein
PDT	Photodynamic Therapy
PpIX	Protoporphyrin IX
SMA	SubMiniature version A
TEC	Thermoelectric Cooler
YFP	Yellow Fluorescent Protein
5-ALA	5-Aminolevulinic Acid

1. INTRODUCTION

Nowadays fluorescence is utilized widely in many fields of science, such as biochemistry, medicine and analytical chemistry. In life sciences, fluorescence is often the preferred analytical method, since it is a non-destructive way to study delicate organisms as opposed to approaches based on radioactivity, for example.

Fluorescence happens also intrinsically in the nature, in a phenomenon known as biofluorescence. Certain species of marine animals such as sharks can produce and sense biofluorescent light which they use for both communication and mating. These glow-in-the-dark sharks, portrayed in Fig. 1, can give their thanks to fluorescent proteins and special intraocular filters in their eyes, allowing them to emit and see fluorescence in the challenging conditions of the sea.

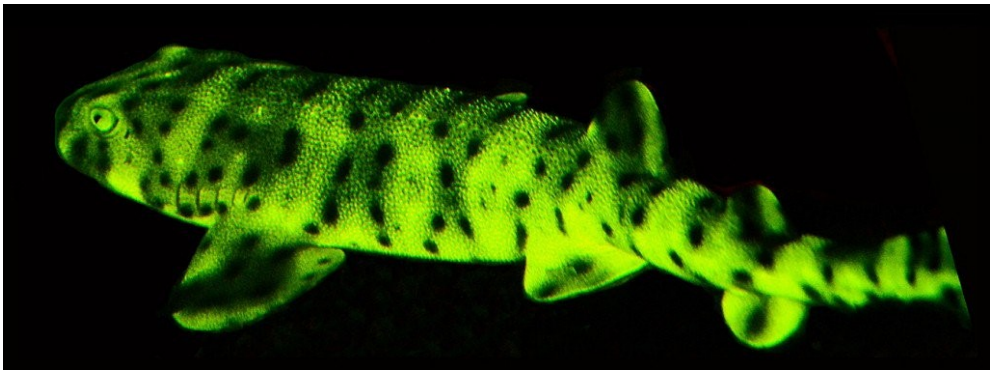

Figure 1. *Biofluorescent swell shark. Available at: https://owlcation.com/stem/Biofluorescence-Colored-Light-Emission-by-Marine-Animals. Accessed Mar 9, 2019.*

Devices, capable of inducing and measuring fluorescence, are currently one of the key research tools used when carrying out in vitro studies. It is therefore appealing for companies in this field to develop devices with integrated fluorescence measurement systems to better satisfy customer needs in their research.

The aim of this thesis is to begin the product development of a fluorescence measurement system for a multi-well plate illumination device, manufactured by Modulight Inc.,

by constructing a measurement setup inside the illumination device and testing its functionality in practice with fluorescence measurements. Modulight Inc. manufactures medical laser devices for clinical and research purposes used, for example, in the treatment of cancer and the research of photoactivated drugs. Offering this type of illumination device with an integrated fluorescence measurement system could increase the device's appeal and expand its customer base.

The structure of this thesis is the following. In Chapter 2, the principles of fluorescence as a physical phenomenon are covered briefly, as the focus of the thesis lies in the experimental part. In addition, the methods to excite and measure fluorescence, microplate readers, optical filters and fluorophores are discussed. In Chapter 3, the constructed setup and the prepared samples for the fluorescence measurements are presented and accounted for. The results of these measurements are presented in Chapter 4. Finally, in Chapter 5, the results are analysed to evaluate the performance of the built setup and ideas for future development are proposed.

2. FLUORESCENCE SPECTROSCOPY

2.1 Principles

Fluorescence is a physical phenomenon during which photons are emitted by a substance that has previously absorbed photons from a light source. This, however, is a general description for an event known as photoluminescence which can be divided into two categories, namely fluorescence and phosphorescence. The way these two differ is in the time it takes for the photons to be emitted after the light has been absorbed by the substance. In fluorescence this time is very brief, of the order of nanoseconds, whereas in phosphorescence the emission of light takes much longer, happening in the course of microseconds up to even milliseconds or seconds, depending on the substance. [1, p. 2476]

These two types of emissions result from different excited states of the electron in a substance. In the case of fluorescence, the electron, which has been lifted to the excited orbital by means of the absorbed energy from the photon, has the opposite spin compared to its pair, located at the ground state orbital. This state is known as the excited singlet state. As a result of obeying Pauli exclusion principle, the electron has an unobstructed return path to its ground state since electron pairs in orbitals are required to have the opposite spin to each other [2]. The electron's return results in an emitted photon, which we identify as fluorescence. Phosphorescence, on the other hand, occurs when the excited electron's spin is the same as its pair in the ground state, a state known as the excited triplet state, preventing the electron's rapid return and resulting in longer emission times. [3, p. 1]

In both cases, the energy of the emitted photon is always lower than that of the absorbed one. These changes in energy can be observed from the Jablonski Diagram, illustrated in Fig. 2.

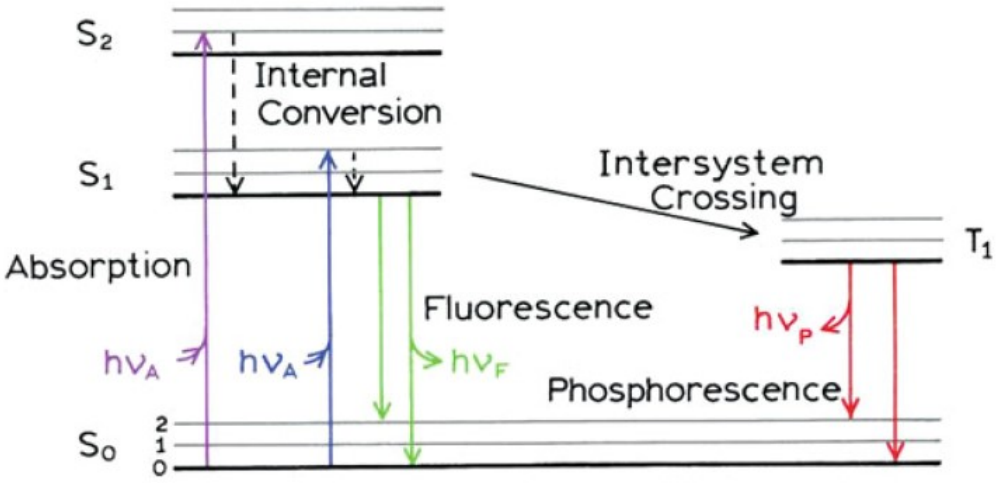

Figure 2. *Jablonski Diagram illustrating the energy levels of a substance. The thicker horizontal lines are located at ascending energy levels, starting from zero at the ground state S_0. The vertical distance between each line corresponds to the energy difference between the levels. The thinner horizontal lines signify the vibrational energy levels, differing only slightly from the nearest electronic states. [4, p. 3]*

As described before, in fluorescence, the absorbed energy from the photon moves the electron to an excited singlet state, here depicted as S_1 and S_2. This transition can only occur if the photon's energy is equal to the energy difference between the ground state and the excited state. Therefore, the light used to excite the substance must be of specific wavelength, as wavelength is inversely proportional to the photon's energy [5, p. 1060–1061]. However, the existence of vibrational levels allows the substance to be excited not only by a single wavelength, but rather a band of wavelengths close to the before mentioned energy difference. Consequently, each fluorescent substance, also known as fluorophore, has their own characteristic absorbance spectrum, depicted in Fig. 3.

Generally, when the fluorophore is excited, the electron reaches one of the many vibrational levels of S_1 or S_2. After this, in most cases, an event known as internal conversion takes place, shown in Fig. 2, during which the electron descends down to the lowest vibrational level of S_1 in a matter of picoseconds, dissipating the excess energy into its surroundings [3, p. 5–7]. Compared to the nanosecond timescale it takes for the fluorescence to occur, internal conversion happens much quicker, and therefore typically fluorescence emission photon is produced by an electron falling down to the ground state from the lowest vibrational state of S_1, as internal conversion has already had the time to take place.

There are also vibrational levels around the ground state, meaning that the emitted light consists of a band of wavelengths, forming an emission spectrum similar to absorption, shown below in Fig. 3. Even so, in some fluorophores, such as in single atoms or monatomic ions, no vibrational levels exist, and therefore the ideal emission spectrum contains only a single wavelength [4, p. 5].

It is also possible for an excited electron at S_1 to experience something known as spin conversion, transforming from first singlet state S_1 into the first triplet state T_1, also shown in Fig. 2. From this position, returning to ground state will generate a phosphorescence photon of longer wavelength than that of fluorescence photon. This event is known as intersystem crossing.

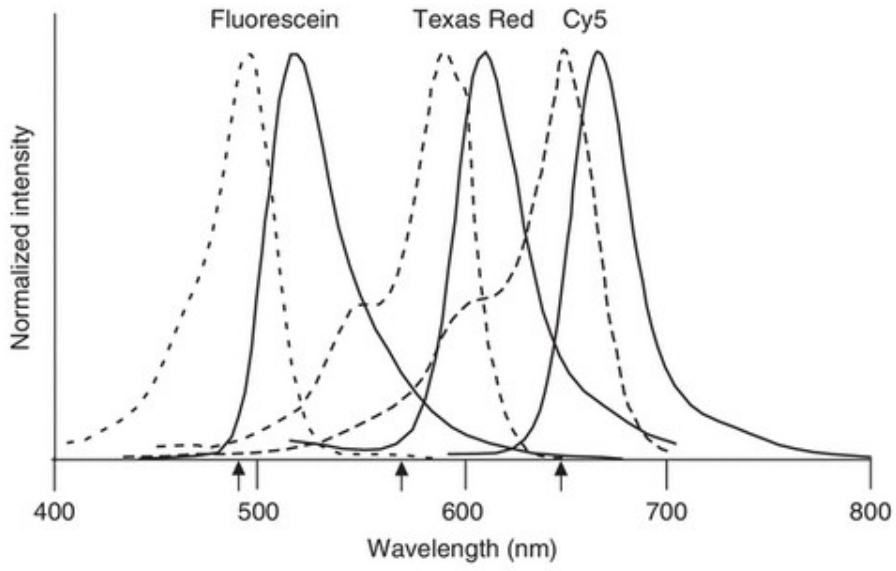

Figure 3. *Fluorescence absorption and emission spectra of three different fluorophores: fluorescein, Texas Red and Cy5. The dotted lines represent absorption wavelengths and full lines emission wavelengths respectively. [6, p. 90]*

In Fig. 3 it can be seen that emission wavelengths are always longer than those of absorption. This is known as the Stokes shift which is defined as the gap between the maximums of the absorption and emission band, usually expressed in wavenumbers [7, p. 72]. When conducting fluorescence measurements, the larger the Stokes shift is, the easier it is to differentiate whether the detected photons are actual fluorescence or from the light used to excite the substance.

2.2 Fluorescence Measurement System

2.2.1 System Design

Fluorescence spectroscopy focuses primarily on the measurement of the following parameters from a sample:

- excitation source spectrum,
- fluorescence emission spectrum,
- fluorescence lifetimes, also known as decay times,
- quantum yield,
- polarization of light, also known as anisotropy. [1, p. 2476]

Of these five parameters, the first two can be measured in a rather straightforward manner using a setup with a commercial spectrometer as the fluorescence detector which generates a spectrum of the light's intensity as a function of wavelength, similar to Fig. 3 [8].

Instruments that are capable of measuring emission and excitation spectra are termed as spectrofluorimeters, whereas those that measure the fluorescence lifetimes are called spectrofluorometers. These terms are often mixed up, since nowadays there are instruments that can measure both the spectra and the lifetimes. For this reason, in this thesis, the term spectrofluorometer will be used when discussing the whole measurement system, whereas the term spectrometer is used to refer to a component of the system, its function being the detection of light.

What is common for a typical spectrofluorometer is that it contains a light source, optical filters or monochromators, and a light detector. The spectrofluorometer also contains optics used for the collimation of excitation light beam and the collection of fluorescent light to the spectrometer. This type of setup, using filters, is illustrated in Fig. 4.

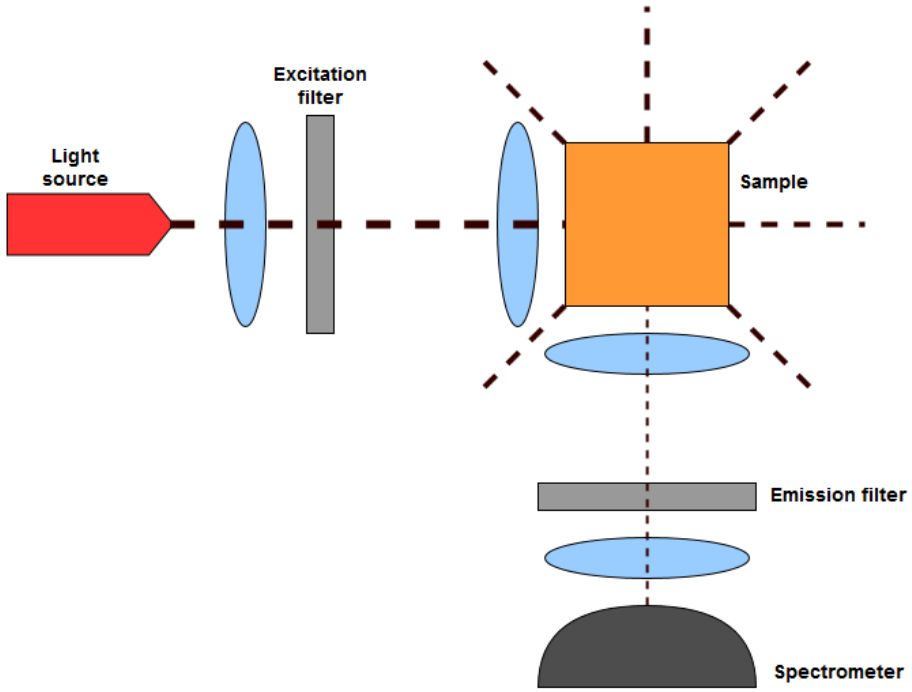

Figure 4. *Typical spectrofluorometer design using optical filters.*

Choosing between a design with filters or monochromators partly depends on which type of light source is selected. In the above design, which is based on filters, an obvious choice would be a laser, since it can emit a narrow spectrum of light, allowing the fluorophore's excitement to happen respectively at a narrow wavelength range. The excitation filter is used to limit this range down to even a greater extent. The emission filter, on the other hand, determines which wavelengths reach the detector by letting the maximum amount of fluorescent light through while blocking most of the stray light from the excitation light source thus improving signal-to-noise ratio.

Monochromator-based designs typically use xenon arc lamp as the light source which emits a continuous spectrum from approximately 250 nm up to 1200 nm, shown in Fig. 5.

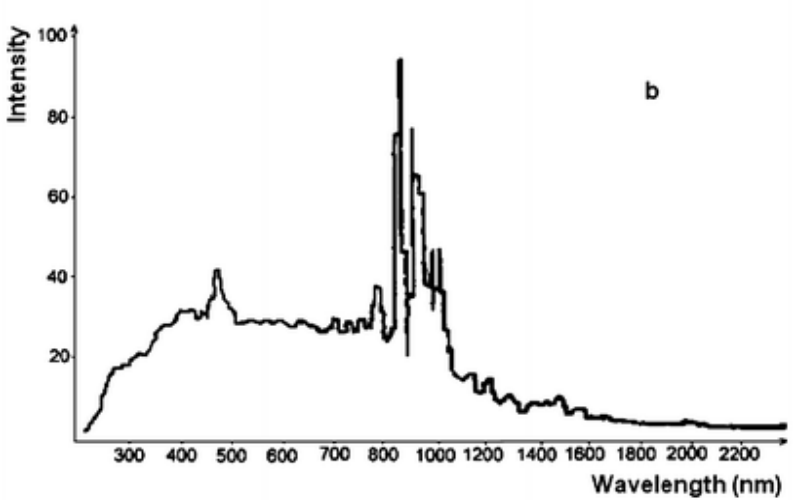

Figure 5. *Spectrum of a xenon arc lamp [9].*

In the case of the above type of excitation spectrum, a monochromator can be used to select the correct wavelength band needed for the excitation of the fluorophore. A second monochromator is used right before the detector to filter out the wavelengths which are not actual fluorescence, but stray excitation light or light from other sources external to the system.

Compared to the rather bulky monochromators, optical filters are much simpler and smaller, typically consisting of pieces of glass with thin-film coatings or doped with absorptive molecules, making them also more affordable [4, p. 6]. Optical filters are discussed in more detail in Chapter 2.2.2.

Regardless of which design is selected, one critical design choice should be considered. By placing the light detector at a 90° angle with respect to the excitation source's beam of light, as is done in Fig. 4, the signal-to-noise ratio can be greatly enhanced as the amount of background noise is reduced, which is caused by the excitation light reaching the detector [1, p. 2479].

2.2.2 Optical Filters

The main function of an optical filter is to transmit light of only certain wavelengths while obstructing other wavelengths from traversing through. These filters typically function as high-pass, low-pass or band-pass filters. The first one transmits wavelengths that are longer than a certain cut-on wavelength, at which point the transmission increases to 50 % through the filter. The second one functions in an opposite manner, allowing the wave-

lengths that are shorter than the cut-off wavelength, i.e. where the transmission decreases to 50 %, to pass through. Both high-pass and low-pass filters transmit wavelengths above and under the cut-on and cut-off point, but these points are often used to describe their effective filtering range. Band-pass filters, on the other hand, transmit bands of wavelengths, for example wavelengths from 600 nm up to 700nm. This chapter discusses optical filters based on two different designs: the first type of filters are based on absorption, known as absorptive filters, and the second type is based on reflection, called dichroic filters, which are also referred to as thin-film filters.

Absorptive filters are typically made either from glass that has been dyed, or from pigmented gelatine resins. Their working principle is that the dye, which is located inside the glass or gelatin, functions as an absorber, attenuating other wavelengths while letting others pass through. By having the filter process happen inside the component rather than on the surface, absorptive filters are far less sensitive to scratches and other surface damage than dichroic filters. Another advantage compared to their counterparts is that absorptive filters are indifferent to the angle of incidence of the input light, experiencing only small differences in absorption due to a changing optical path if the filter is placed at an angle relative to the incident light. [10]

Whereas absorptive filters absorb the undesired wavelengths, hence the name, dichroic filters rely on reflecting these wavelengths. In this way only the the desired portion of the spectrum is transmitted. They are based on coated thin-film layer structures, which are made of thin, flat and parallel layers with variable thicknesses ranging from few ångströms to tens of micrometres. These layers, consisting for example from titanium dioxide and silicon oxide, can be manufactured by evaporating the desired structure layer by layer on a substrate using a technique called electron beam evaporation [11, p. 7, 12–13]. What causes this ability to reflect some wavelengths and transmit others are thin-film interference phenomena which take place at the interfaces of the coated layer structure. Dichroic filters offer better filtering capabilities compared to absorptive filters, and since they reflect the light instead of absorbing it, dichroic filters do not heat up as much as the absorptive ones under illumination. However, thin-film coatings are designed for a specific angle of incidence of the incoming light, typically at normal incidence for band-pass, low-pass or high-pass filters and at 45° angle for beam-splitters. [12]

2.2.3 Microplate Readers

Microplate readers, commonly known as plate readers, are analytical instruments capable of performing spectroscopic studies for multi-well plates, which typically consist of 6, 12, 24, 48, 96, 384 or 1536 wells per plate, laid out in a rectangular matrix with a ratio of 2:3. An example of a 96-well plate is shown in Fig. 6. Depending on the indication, plate readers can be constructed to detect and analyse, for example, fluorescence, absorbance or radioactivity. They are often equipped with an atmospheric control system for the samples, allowing the regulation of temperature and O_2 and CO_2 levels. [13] One type of plate reader, manufactured by BMG LABTECH GmbH, is illustrated in Fig. 6.

Figure 6. *A 96 well plate, showing both the top and bottom view and the lid, manufactured by Cellvis [14] (left). FLUOstar® Omega microplate reader, manufactured by BMG LABTECH GmbH (right) [15].*

A plate reader that can measure fluorescence intensity partly follows the design shown in Fig. 4 and contains an excitation system which produces either a narrow spectrum using a laser or a broadband spectrum with a xenon arc lamp, both of which are then filtered by using optical filters or monochromators. Emitted fluorescence is detected as it passes through the emission filters and to the light detector, as discussed in Chapter 2.2.1.

Microplate readers, however, cannot directly make use of the 90° angle layout, which would improve signal-to-noise ratio, because the well plate must be in a horizontal position at all times to keep the samples contained within the wells. Therefore, although the components of the measurement system stay nearly the same, their positioning must be

altered. Commercial microplate readers can be classified according to where the fluorescent light is detected relative to the well plate; from the top, bottom or the ability to choose from either one. The multiple arrangement choices result from different research demands; detecting fluorescence from the top yields a better signal-to-noise ratio in solution-based samples, because the detected fluorescent light does not travel through the plastic material of the well plate, which would attenuate and scatter the light, and therefore weaken the detected signal. Yet in some studies, such as those conducted with adherent cells which grow at the bottom of the plate, detecting fluorescence from the bottom can produce better results. [16] The optical path, i.e. the route the light travels from its source to the detector, in a top-detecting plate reader is shown in Fig. 7.

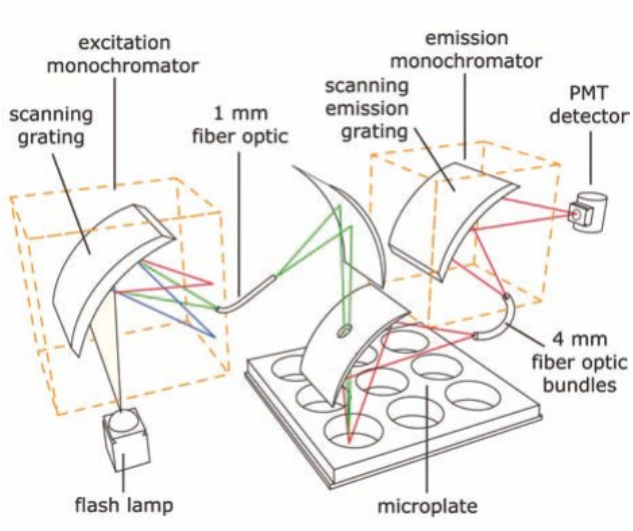

Figure 7. *Top-detecting microplate reader's optical path [3, p. 30]*

The above type of design uses monochromators for both excitation and emission light. Due to the nature of fluorescence, the fluorescent light is emitted in all directions from the sample in the well, and therefore it is possible to use a mirror with a hole in it, through which the excitation light can pass to the sample, while the same mirror guides the emitted fluorescent light to the detector. Using clear-bottomed well plates, such as the one shown in Fig. 6, allow for a more simple design, since the light can be targeted at the well directly under the well plate, reducing the number of mirrors needed. This in turn results in minor losses in the intensity of the excitation light, because it travels through the plastic well plate. Although not shown in Fig. 7, plate readers are usually equipped with x-y linear travel stages which enable the device to perform measurements on each well independently by changing the well plate's position while the optical system stays fixed.

The automated multi-well plate illumination device, which is in the focus of this thesis, is primarily intended for the illumination of well plate samples. It is therefore not practical to compare it to plate readers in terms of measurement capabilities as they serve a different purpose. However, the design of the plate readers' fluorescence intensity measurement can be utilized to an extent in the development of the illumination device.

2.2.4 Spectrometers

Spectrometers serve as analytical tools to separate light into its spectral components which can then be presented to the user in terms of intensity as a function of wavelength. This chapter provides insight into how spectrometers function and hence how they can be used as a component in the fluorescent measurement system. Although commercially available, it is sensible to know the working principle of a spectrometer rather than merely take it as a black box -component. The contents of a typical spectrometer are shown in Fig. 8.

A typical spectrometer consists of three distinct segments: the entrance slit, the diffraction grating and the detector. Together they form an optical assembly, also referred to as the spectrograph or the optical bench. The spectrometer also contains a fiber input port, which is usually configured for a common fiber connector type, such as the Sub Miniature A (SMA 905) or Ferrule Connector (FC). Frequently used fiber connector types are illustrated in Fig. 8.

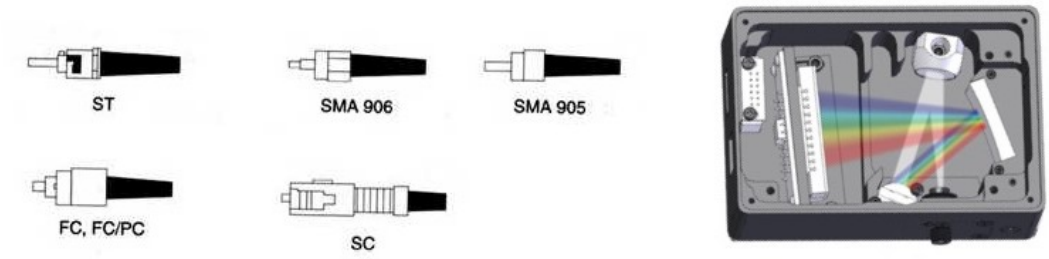

Figure 8. *Common fiber connector types (left) [17]. Inner components of a typical spectrometer (right), adapted from [18].*

The main function of the entrance slit is to determine the amount of light let in to the spectrometer, greatly affecting the spectral resolution and throughput of the device. The spectral resolution of a spectrometer can be defined as the maximum amount of spectral peaks that can be individually detected in certain wavelength range. In other words, if a

spectrometer has a 150 nm wavelength range and a spectral resolution of 1 nm, it can detect 150 individual wavelengths at most per measurement. In addition to regulating the amount of light let in, the slit is also used to focus the input light and to control its angle. Slits are qualified in terms of slit width from 5 µm up to 800 µm, and choosing the correct size for the application at hand means balancing between the spectral resolution and throughput of the system.

After entering the spectrometer through the entrance slit, the light is guided with mirrors to the diffraction grating, which ultimately determines the wavelength range of the spectrometer and has an effect on the spectral resolution as well. The purpose of a diffraction grating is to separate light into its spectral components. This is done by diffracting different wavelengths at their corresponding angles, determined by the diffraction equation

$$dsin(\theta_m) = m\lambda \tag{1}$$

where d is the distance between the grating grooves, θ_m is the angle between the normal vector of the grating and the diffracted ray, m is an integer referring to the order of maxima in which the phases add together and λ is the wavelength of the incident ray. [19]

There are two types of diffraction gratings, namely ruled gratings and holographic gratings. The former gratings consist of parallel grooves etched on the substrate's surface and coated with a reflective material, while the latter is made using two interfering UV light sources which generate sinusoidal variation in the index of refraction in an optical glass used as a base for the component. Choosing a correct grating type is a matter of cost and stray light efficiency, because ruled gratings are less expensive but they contain small imperfections in the grating, increasing the amount of stray light emitted. Holographic gratings possess two key advantages. The first one is that their manufacturing process is less prone to errors, resulting in only a small amount of emitted stray light. The second feature is that holographic gratings can be applied to non-planar surfaces so that the created component can serve simultaneously as a diffraction grating and an optic for focusing.

The detector of a spectrometer is nowadays often laid out as a Charge-Coupled-Device (CCD) array, so that the light, dispersed into its wavelength-components by the diffraction grating, can hit the individual pixels of the array, providing a configuration where the intensity measured from a pixel corresponds to a specific part of the spectrum. This information is then used to create a full spectrum of the input light, displaying the intensity

as a function of the wavelength. A design based on this arrangement contains no moving parts, thus allowing the spectrometer to be downsized and operated with less power. It should be noted that pixel width and the number of pixels in the array both have an effect on the spectral resolution of the spectrometer. [18]

The data measured by the spectrometer's CCD array contains noise which consists of the following types:

- read noise
- shot noise
- fixed pattern noise. [20, p. 21]

Read noise is a combination of various noise types, such as dark current noise and ADC quantizing noise, to name a few. The former is caused by the CCD's pixels generating charge without photons striking the detector, hence the noise type's name. Dark current noise is temperature dependent, as more thermal electrons are generated with the rise of detector temperature, adding to the noise level. In order to reduce dark current noise, the CCD array can be cooled with a thermoelectric cooler (TEC). The latter noise type occurs during the signal digitization, as the quantization process involves uncertainty. All in all, read noise is signal independent and forms a baseline for the total noise level of the detector.

Shot noise is related to photon interaction and results from the way photons arrive on the detector's pixels; photon's probability to strike a pixel follows the Poisson distribution. This type of noise is proportional to the square root of the input signal.

Not all pixels of the CCD array are equal in terms of photon collection efficiency. This results in fixed pattern noise. The term "fixed" results from variations in the pixels' structural properties and therefore the resulting noise stays the unchanged, i.e. fixed, on each measurement. Moreover, fixed pattern noise is proportional to the signal, contributing to a greater proportion of the total noise than shot noise.

2.3 Fluorophores

Fluorophores are chemical compounds with the ability to emit fluorescent light upon excitation with specific wavelengths of light, range of which is characteristic to each substance's molecular structure [21]. There are main types of fluorophores, namely intrinsic

and extrinsic. Intrinsic fluorophores, such as aromatic amino acids, occur naturally without the need of artificial modification. Extrinsic fluorophores, such as fluorescein, on the other hand, are substances added to the sample when there are no intrinsic fluorophores readily available, or their fluorescent capabilities are not sufficient. [3, p. 63] In this chapter, common fluorophores such as green fluorescent proteins and fluorescein will be discussed. Protoporphyrin IX will be addressed as well, as it is used in the experimental part of this thesis. It is used due to its availability and suitable excitation and emission spectra.

Green fluorescent protein (GFP), its structure shown in Fig. 9, is a protein with an internal fluorophore. GFP can be found in nature and it was originally extracted from a jellyfish species Aequorea victoria. Its fluorescent capabilities result from its chemical structure, where through appropriate folding, which is characteristic to protein structures, three amino acids covalently rearrange and molecular oxygen is oxidized, creating an internal fluorophore. If this formed structure is isolated from the whole protein, it does not elicit fluorescence, because it lacks the correct folding provided by the polypeptide chain of the protein backbone. GFP has two distinct excitation peaks, which result from two possible forms of the fluorophore's structure, illustrated in Fig. 9. The fluorophore's excitation happens at 395 nm and 475 nm, the former being a more prominent peak. Its fluorescence emission is at 509 nm, which is in the green light portion of the visible spectrum, granting GFP its name. It has also been used to create a family of fluorescent mutant proteins similar to GFP's structure, such as the Yellow fluorescent protein (YFP). GFP has had a great impact on biotechnology and life sciences where its derivatives are utilized as fluorescent markers.

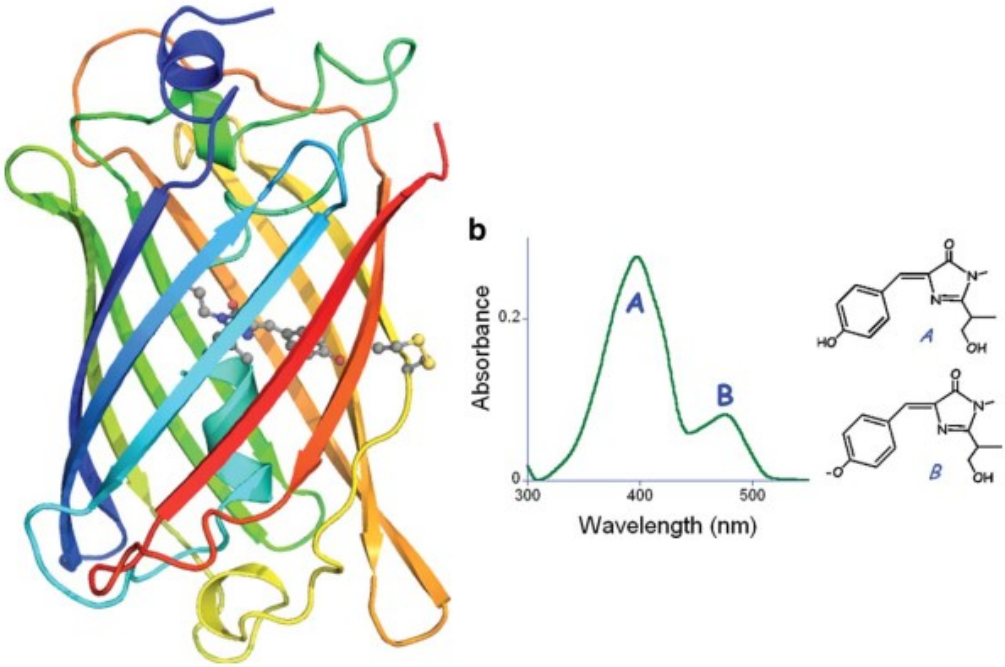

Figure 9. *Green fluorescent protein (left), more specifically a modified version of it, termed roGFP2. The fluorophore structure, which is responsible for the fluorescence is shown in ball and stick configuration in the middle. Excitation spectrum of GFP (right) and neutral (A) and anionic (B) versions of the part of the structure responsible for the excitation peaks. [22]*

Fluorescein, also known as Resorcinolphthalein, is an organic chemical compound named after its fluorescent properties. It emits green fluorescent light at 521 nm when mixed in alkaline solutions and excited with light at 494 nm. Fluorescein has found use in a variety of applications, such as in ophthalmology, where it is used as a diagnostic tool to detect corneal injuries, and the dry areas on the surface of the cornea. Other applications include, for example, usage in lifesaving equipment as a fluorescent tracer dye to spot targets in seawater, or as a fluorescent indicator in acidic solutions, where the rise of pH from 4 to 4,5 can transform a Fluorescein-containing solution from colourless to green. [23]

Protoporphyrin IX (PpIX) is a chemical compound belonging to a group of organic heterocyclic macrocycle compounds. It is a type of fluorophore, found occurring naturally in living organisms, where it acts as a precursor to hemoglobin in vertebrates and chlorophyll in plants and algae [24]. The chemical structure of Protoporphyrin IX is illustrated in Fig. 10. As is characteristic to porphyrin derivatives, the most notable fluorescent peak of PpIX at around 400 nm is due to the transitions the in π-bonds, made possible by the electron dipole movement in the structure. This peak is known as the Soret band maximum [25]. The typical absorption and emission spectra of PpIX are shown in Fig. 10.

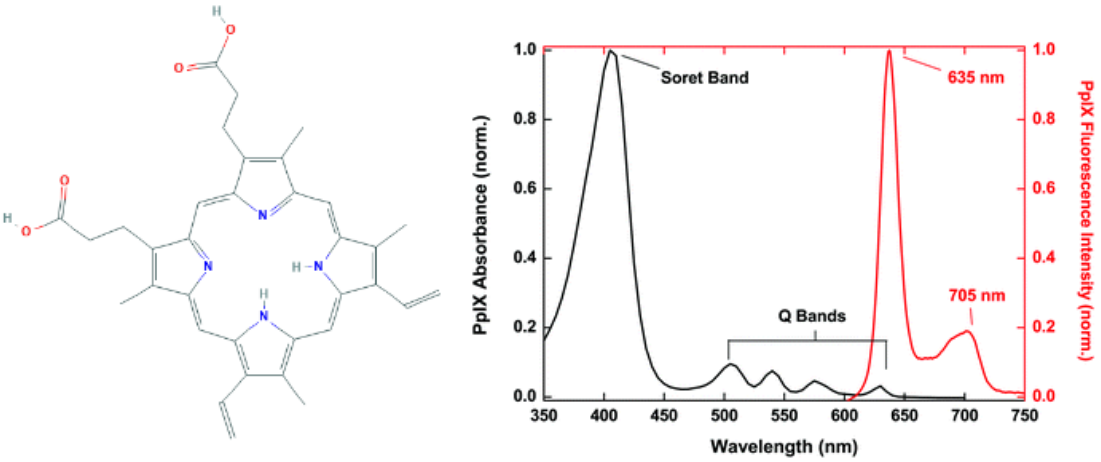

Figure 10. *The chemical structure of PpIX (left) [26]. PpIX excitation and fluorescence emission spectra (right) [27].*

As can be seen from Fig. 10, PpIX is maximally excited with wavelengths around 400 nm and the most prominent emission peak is located at 635 nm. However, in medical indications, such as in fluorescence-guided surgery, this excitation peak may prove to be unusable, as tissue penetration of the light at shorter wavelengths is low due to the high absorption of the excitation light by hemoglobin (Hb) and oxyhemoglobin (HbO_2) [28, p. 1690]. To cope with this, the other excitation peaks of PpIX, marked in Fig. 10 as the Q Bands, can be exploited. In this situation, PpIX is illuminated with red light at 620–640 nm, and fluorescence emission can be detected at wavelengths around 700 nm. Fig. 11 illustrates the before mentioned red light illumination absorption and emission spectra of PpIX and depicts how Hb and HbO2 absorb the light at the lower wavelengths, around 400 nm.

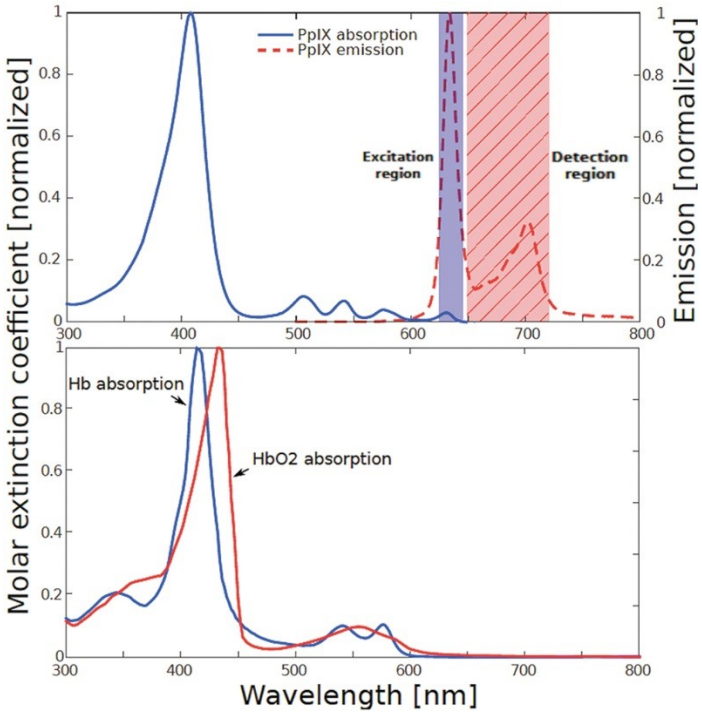

Figure 11. *Red light illumination absorption and emission spectra of PpIX and absorption spectra of Hb and HbO_2 [28, p. 1691].*

In addition to fluorescence-guided surgery, other uses of this compound include the stimulated formation of PpIX in the tissue using 5-aminolevulinic acid (5-ALA) which is followed by light excitation to eliminate surrounding cancer cells. This is an essential part of the treatment known as photodynamic therapy (PDT). With this therapy, patients suffering from various types of malignant or non-malignant tumours can be treated.

The treatment begins with the administration of the photosensitizer. After this, the drug starts to accumulate in the treatment location. However, the accumulation efficacy varies between different photosensitizers, resulting in the accumulation of the photosensitizer to non-targeted sites, such as organs, liver being the most common localization site [29]. 5-ALA is used as a precursor drug (prodrug), to locally promote the production of PpIX, which can then be excited with wavelengths from 620 nm to 640 nm, as described above. This excitation allows for the tissue oxygen, which otherwise exists in the triplet state, to be transformed into the singlet state through intersystem crossing. As a result, the singlet state oxygen, which is highly reactive, attacks the neighbouring cells causing them to undergo necrosis. [30] Due to the short lifetime of singlet state oxygen, the effect of this treatment is local and targeted as opposed to many other cancer treatments such as chemotherapy.

3. METHODS

The aim of the experimental part of this thesis is to propose a fluorescence measurement system design for the automated multi-well plate illumination device, manufactured by Modulight Inc. This device, shown in Fig 12, is marketed under the name of ML8500 – an automatic biomedical illumination system. It is used by researchers in in-vitro studies to provide rapid, accurate and sequential illumination of multi-well plate samples. [31]

Figure 12. *ML8500, automatic biomedical illumination system, shown from the front.*

The illumination system contains an integrated positioning system for the inserted well plate. This allows the well plate to be moved inside the system, thereby making it possible to illuminate the selected wells. For this reason, the fluorescence measurement system can be a fixed setup, so that the well plate is the only moving component. The system also functions as a platform on which the various components of the measurement system can be attached.

Other advantages provided by the illumination device are that it is cloud-connected, making it possible to create illumination protocols, depicted in more detail later in this chapter. Moreover, Modulight's other laser systems can be connected directly to ML8500's internal control unit and therefore acquiring the correct wavelength for the application is a straightforward task by connecting a laser system with a suitable configuration.

The measurement setup was constructed using the following components:

- excitation light source
- collimation lens and a beam homogenizer
- 96-well plate with varying concentrations of PpIX
- lens for the fluorescence collection
- filters for the excitation light
- a commercial spectrometer.

The component layout followed the design of Fig. 4 to some extent, but as described in Chapter 2.2.3, there were limitations to the design set by the placement of the well plate and therefore the design had to be modified. A schematic showing the component placement in the measurement setup is illustrated in Fig. 13. The design made use of the internal connection points provided by the illumination system and was constructed so that it could be fitted inside the device.

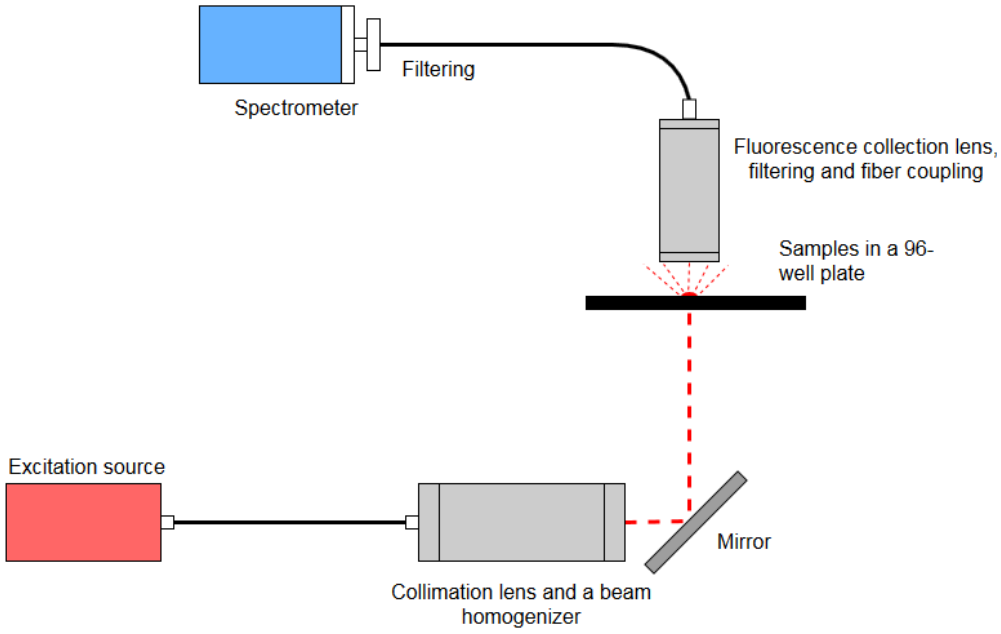

Figure 13. *Constructed fluorescence measurement setup.*

A laser system manufactured by Modulight, marketed under the name of ML6600, was used as the light source for the excitation of the samples. It provided a narrow (± 1 nm) excitation wavelength band, peaking at 636.3 nm. This was very close to the target wavelength of 635 nm, which is the excitation peak of PpIX. The spectrum of the excitation light source is shown in Fig 14.

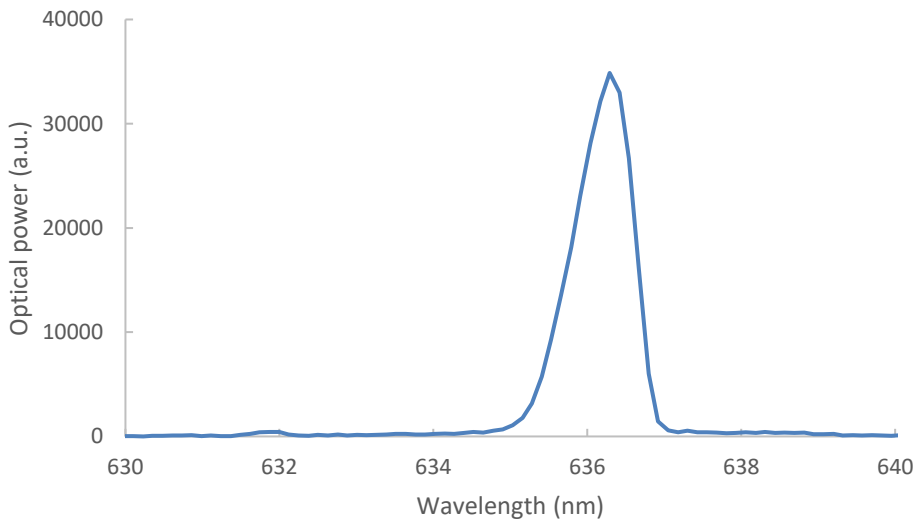

Figure 14. *Spectrum of the excitation laser source, showing a peak wavelength at 636.3 nm.*

The excitation light was guided from its source with an optical fiber to the collimation lens. The collimation was done in order to direct the excitation light through the system with only little divergence and in this way reduce optical power losses due to beam divergence. After this, the beam was homogenized to receive a suitable light distribution at the sample well plate. Lastly, before arriving at the sample, a mirror was placed in front of the beam at a 45° angle to illuminate the sample from the bottom.

To allow for the detection of fluorescence, a lens was placed above the sample to increase the collection of the emitted fluorescent light while an absorptive filter was used to reduce the collected excitation light. After this, the light was fiber-coupled and directed towards the spectrometer, but in order to filter out the excitation light even further, a dichroic filter was placed right before the spectrometer.

For the sample, a PpIX solution with the concentration of 1 g/l or 1.78 mM was prepared by measuring 10 mg of PpIX and dissolving it to 10 ml of dimethyl sulfoxide (DMSO). This solution was then used to create an 8-step half-logarithmic serial dilution, resulting in a dilution factor of $10^{0.5}$ (approximately 3.16), using distilled water as the diluent. The concentrations for all of the dilutions are shown in Table 1.

Table 1. *PpIX concentrations for the 8-step half-logarithmic serial dilution. The ordinal numbers denote the number of dilutions and the letters correspond to which row of the well plate this concentration was pipetted.*

Dilutions	ρ (mg/l)	c (µM)	Well plate row
1	1000	1777	A
2	316	562	B
3	100	177	C
4	31.7	56.1	D
5	10.0	17.7	E
6	3.17	5.60	F
7	1.00	1.77	G
8	0.318	0.559	H

After preparation, the different concentrations were pipetted in a well plate, depicted in Fig. 15. This was done in such a manner that the concentration remained the same for all 12 columns of the well plate (marked on the well plate as numbers 1, 2, 3, …, 12), but varied from row to row, as shown in Table 1, starting from the strongest concentration in row A and ending in the lowest concentration in row H.

Figure 15. *Half-logarithmic serial dilution of PpIX pipetted on a 96-well plate.*

As can be seen from the above picture, a black well plate with a clear bottom was used in order to reduce cross-illumination between the individual wells. For all 96 wells, the pipetted volume of PpIX solution was 180 µl.

The purpose for this type of arrangement was to measure the effect of fluorophore concentration on the detected fluorescence intensity. In addition, by having 12 identical wells for each concentration, it was possible to alternate the intensity of the excitation light and see how it affects the detected fluorescence emission intensity. An illumination program was created by using Modulight's cloud-based software to carry out the measurement. With this program, a specific intensity and a light dose could be selected for all 12 columns. The light dose can be calculated with the following equation:

$$Dose\ \left(\frac{\mathrm{J}}{\mathrm{cm}^2}\right) = Intensity\ \left(\frac{\mathrm{W}}{\mathrm{cm}^2}\right) \cdot Time\ (\mathrm{s}). \tag{2}$$

By choosing a fixed illumination time of 5 seconds for all the wells, the intensity could be increased from column to column, resulting in increasing doses. The parameters for the program are shown in Table 2.

Table 2. *Intensities and doses used in the illumination protocol for all 12 columns.*

Column	I (mW/cm^2)	Dose (J/cm^2)	Time (s)
1	200	1	5
2	300	1.5	5
3	400	2	5
4	500	2.5	5
5	600	3	5
6	700	3.5	5
7	800	4	5
8	900	4.5	5
9	1200	6	5
10	1500	7.5	5
11	2000	10	5
12	2500	12.5	5

The constructed measurement setup in combination with the illumination program resulted in a measurement arrangement which, for the prepared the 96-well plate, could measure an emission spectrum from each well, generating a total of 96 spectrums per measurement run. The results gained from these measurements are presented in the next chapter.

4. RESULTS

The measurements were performed two times by changing the integration time of the spectrometer in between. The used integration times were 10 ms and 50 ms. Increasing this time allowed the spectrometer to capture light for a longer duration of time which in turn increased the intensity of the captured signal. However, this meant that not only the intensity of the fluorescence signal was increased, but also the signal caused by light from other sources, mainly from the excitation light. The measurement results with both integration times are shown in Fig. 16. Both of the measurements contain 96 spectra measured from the sample with varying excitation intensities and PpIX concentrations, as discussed in Chapter 3.

The results of Fig. 16 show a wide fluorescence band peaking at 700 nm. It can be also seen that, despite of the filtering, the excitation light is detected by the spectrometer at around 635 nm. In addition, measurements with low PpIX concentration and high intensity display a third distinct peak at 670 nm, which is due to the excitation light leaking at longer wavelengths, an effect caused by the dichroic filter.

The effect of the integration time can be easily observed from the results below. As discussed earlier, the intensity of the measured fluorescence is higher with the longer integration time, but so is the signal from the excitation source. This results in the fact that with 50 ms time of integration the spectrometer reaches a saturation point considerably sooner than with 10 ms. The saturation point can be seen from the results as the spectrometer’s inability to measure values above 65000 which causes the horizontal saturation bands at around 635 nm.

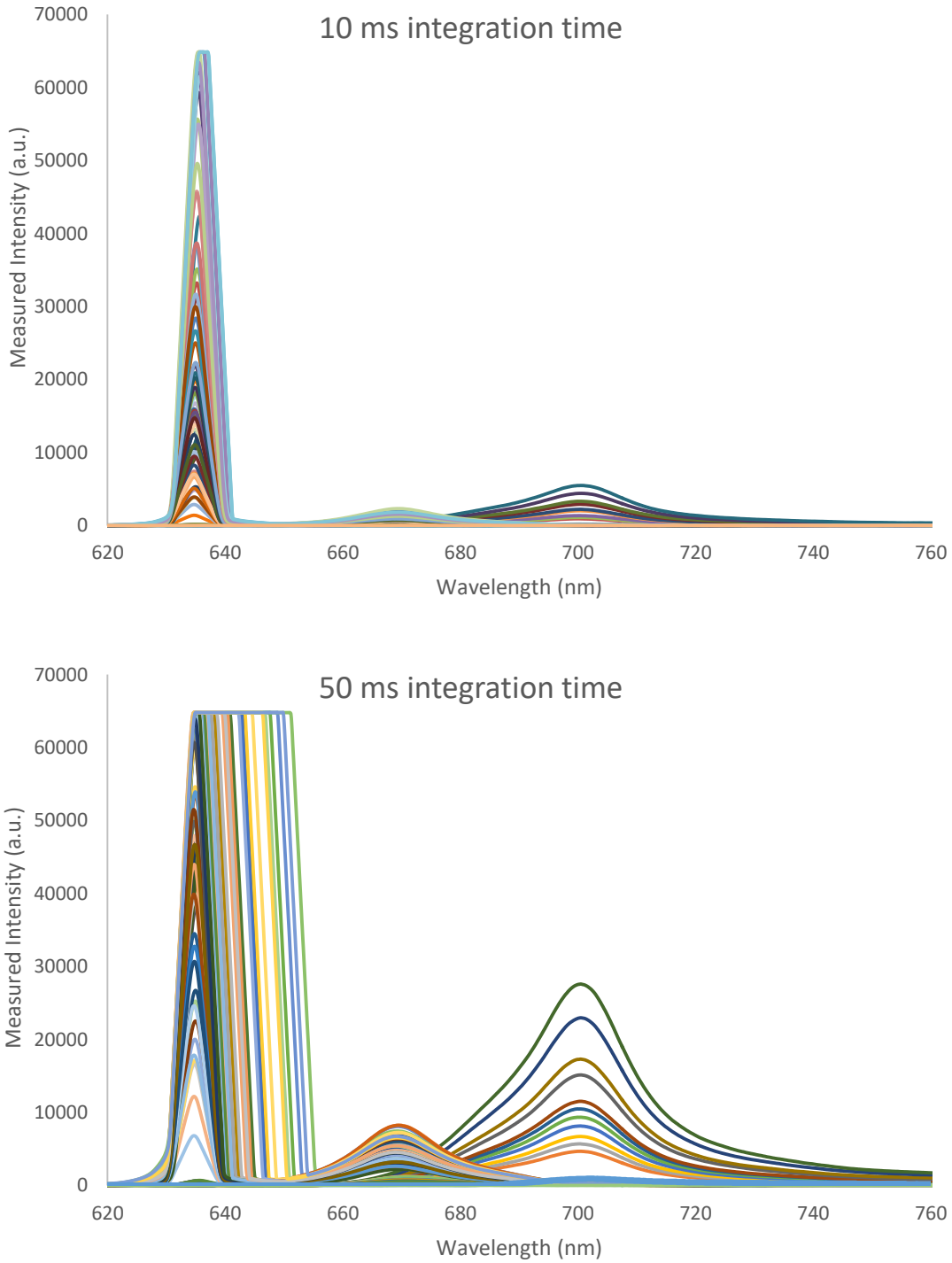

Figure 16. *The spectra measured from PpIX samples under excitation, showing the effect of the integration time.*

The effect of the excitation light intensity on the measured fluorescence intensity is illustrated in Fig. 17 for both 10 ms and 50 ms integration times. These results were plotted from the measured fluorescence intensities at 700 nm with different excitation light intensities at a constant PpIX concentration of 1 g/l. Two data points were excluded from

the 10 ms measurement where no fluorescence signal could be detected, which was most likely due to a random error in the measurement. As can be seen from the image below, the measured fluorescence intensity showcases a linearly dependency on the intensity of the excitation light. However, it can be seen that the first data points with both integration times do not follow this linear dependency. This is caused by the low accuracy of power and intensity of the excitation source due to being close to its lasing threshold.

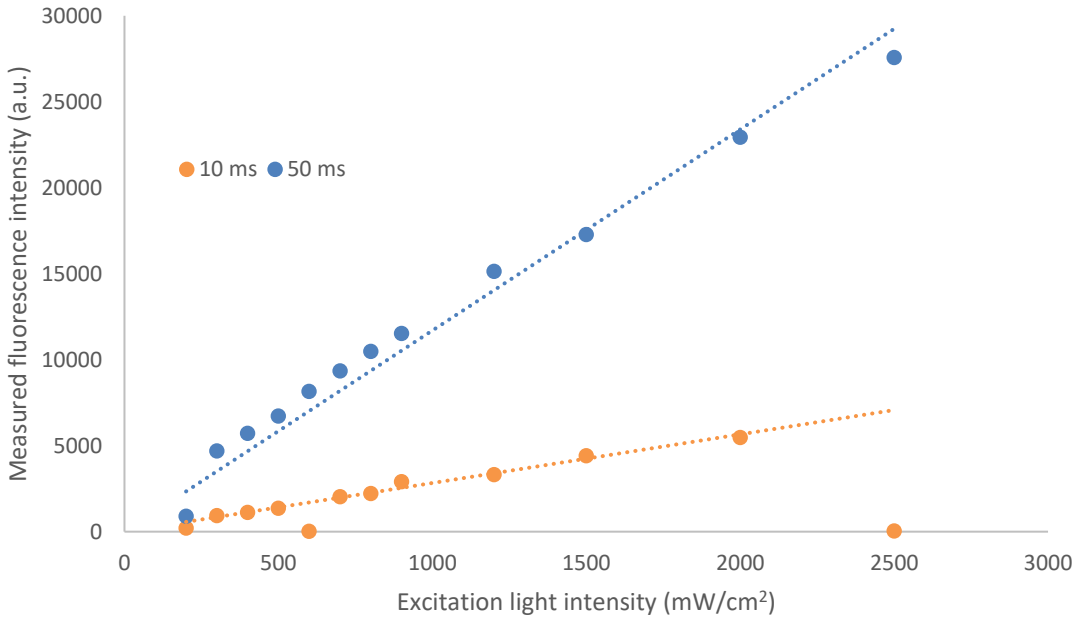

Figure 17. *Measured fluorescence intensity at 700 nm with 1 g/l concentration of PpIX following linear dependency on the excitation light intensity.*

Studying the effect of fluorophore concentration on the detected fluorescence intensity could not be performed as intended, because the dilution factor appeared to be too large. This resulted in that with concentrations smaller than 1 g/l, the excitation light was less absorbed by the sample and therefore caused the spectrometer to reach saturation. The smaller concentrations also meant that there were simply less PpIX molecules to excite, and therefore the emitted fluorescence intensity was negligible and unable to be measured.

5. CONCLUSIONS

In this thesis, a fluorescence measurement system was constructed for the multi-well plate illumination system manufactured by Modulight. The measured spectral results of Fig. 16 displayed similar spectral shapes as is illustrated in Fig. 11, which represents the PpIX fluorescence emission spectrum. Based on these results, the constructed fluorescence measurement system can be considered as a functioning subsystem, which is possible to integrate into the illumination device.

This bachelor's thesis accomplished the targets set to it, i.e. to begin the development of the beforementioned fluorescence measurement system. As a result, the product development of this system has proceeded from a design to a prototype phase, and can be further improved to increase the accuracy and sensitivity of the system.

There are a few ways to develop the system further to better filter out non-fluorescent light and increase the collection of fluorescence from the samples. In order to reduce the amount of detected excitation light signal, the collection optics located on top the sample could be tilted at a small angle instead of directly pointing down towards the incoming excitation beam. This would be possible since fluorescence is emitted in all directions from the sample whereas the excitation light is a collimated laser beam. Additionally, the collection lens position could be further optimized to enhance fiber-coupling of the fluorescent light and in this way boost the measured fluorescence signal.

REFERENCES

[1] Povrozin Y, Barbieri B. FLUORESCENCE SPECTROSCOPY. Hoboken, NJ, USA: John Wiley & Sons, Inc; 2016. p. 2475–2498.

[2] Pauli exclusion principle. : Encyclopædia Britannica Inc; 2018.

[3] Lakowicz JR. Principles of Fluorescence Spectroscopy. Boston: Springer; 2006.

[4] Geddes CD. Reviews in Fluorescence 2016. 1st 2017 ed. Cham: Springer Verlag; 2017.

[5] Young HD, Freedman RA, Ford AL. University physics with modern physics. 14. global ed. Harlow: Pearson; 2016.

[6] Dobrucki JW. Fluorescence Microscopy. ; 2013.

[7] Valeur B, Berberan-Santos MN. Molecular fluorescence: principles and applications. 2nd; 2. Aufl. ed. Weinheim [Germany]; Chichester, England: Wiley-VCH; 2013.

[8] Spectrometer. Encyclopædia Britannica Online 2018.

[9] Gaudin K, Baillet A, Chaminade P. Application of a xenon arc lamp as a light source for evaporative light scattering detection. Analytical and Bioanalytical Chemistry 2006;384(6):1302–1307.

[10] Molecular Expressions Microscopy Primer: Light and Color - Absorption Filters. Available at: https://micro.magnet.fsu.edu/primer/java/filters/absorption/. Accessed Apr 12, 2019.

[11] Orsila L. Optical Thin Film Technology for Ultrafast Fiber Lasers. : Tampere University of Technology; 2008. Available at: http://urn.fi/URN:NBN:fi:tty-200903031027.

[12] What is a Dichroic Filter? Available at: https://abrisatechnologies.com/2014/10/what-is-a-dichroic-filter/. Accessed Apr 12, 2019.

[13] Microplate Reader. The Dictionary of Cell and Molecular Biology 2013:413.

[14] 96 Well glass bottom plates | Cellvis. Available at: https://www.cellvis.com/_96-well-glass-bottom-plates_/products_by_category.php?cat_id=11. Accessed Mar 23, 2019.

[15] FLUOstar Omega Microplate Reader - BMG LABTECH. Available at: https://www.bmglabtech.com/fluostar-omega/. Accessed Mar 23, 2019.

[16] Bioanalytic BT. What are the benefits of top reading vs bottom reading on my microplate reader? - Life Science Instruments. Available at: https://www.berthold-bio.com/service-support/support-portal/knowledge-base/what-are-the-benefits-of-top-reading-vs-bottom-reading-on-my-microplate-reader.html. Accessed Mar 23, 2019.

[17] Types of Common Fiber Connectors. Available at: https://www.lite-way.com/faq/fiber_connectors.htm. Accessed Mar 28, 2019.

[18] How Does a Spectrometer Work? Available at: http://bwtek.com/spectrometer-introduction/. Accessed March 26, 2019.

[19] Mouroulis P. Diffraction grating. Access Science 2014.

[20] Janesick JR. Photon Transfer Curve. : SPIE Press; 2007. p. 49–78.

[21] Fluorophore. Encyclopedia of Genetics, Genomics, Proteomics and Informatics 2008;1:701.

[22] Remington SJ. Green fluorescent protein: A perspective. Protein Science 2011;20(9):1509–1519.

[23] Fluorescein. Available at: https://pubchem.ncbi.nlm.nih.gov/compound/16850. Accessed Mar 24, 2019.

[24] Uehlinger P, Zellweger M, Wagnières G, Juillerat-Jeanneret L, van den Bergh H, Lange N. 5-Aminolevulinic acid and its derivatives: physical chemical properties and protoporphyrin IX formation in cultured cells. Journal of Photochemistry & Photobiology, B: Biology 2000;54(1):72–80.

[25] Uttamlal M, Holmes-Smith AS. The excitation wavelength dependent fluorescence of porphyrins. Chemical Physics Letters 2008 Mar 1,;454(4):223–228.

[26] Protoporphyrin IX. Available at: https://pubchem.ncbi.nlm.nih.gov/compound/4971. Accessed Mar 14, 2019.

[27] Valentine RM, Ibbotson SH, Wood K, Brown CTA, Moseley H. Modelling fluorescence in clinical photodynamic therapy. Photochemical & Photobiological Sciences 2012 -12-13;12(1):203–213.

[28] Roberts DW, Olson JD, Evans LT, Kolste KK, Kanick SC, Fan X, et al. Red-light excitation of protoporphyrin IX fluorescence for subsurface tumor detection. Journal of Neurosurgery JNS 2018;128(6):1690–1697.

[29] Castano AP, Demidova TN, Hamblin MR. Mechanisms in photodynamic therapy: Part three — Photosensitizer pharmacokinetics, biodistribution, tumor localization and modes of tumor destruction. Photodiagnosis and Photodynamic Therapy 2005;2(2): 91–106.

[30] Leanne B. Josefsen, Ross W. Boyle. Photodynamic Therapy and the Development of Metal-Based Photosensitisers. Metal-based drugs 2008;2008:276109.

[31] ML8500 - automatic biomedical illumination. Available at: https://www.modulight.com/ml8500/. Accessed Apr 13, 2019.